Neoplasma 2024; 71(5): 490–497

doi:10.4149/neo_2024_240527N236

Comparative investigation among fluorescence in situ hybridization, DNA- and RNA-sequencing on detecting MYC, BCL2, and BCL6 rearrangements in high-grade B-cell lymphomas

Fen ZHANG[1,#], Qian CUI[1,#], Haiwei DU[2], Xinze LV[2], Ting HOU[2], Yu CHEN[1], Jie CHEN[1], Jian LIU[1], Jinhai YAN[1], Yanhui LIU[1,*]

[1]*Department of Pathology, Guangdong Provincial People's Hospital, Guangdong Academy of Medical Sciences, Southern Medical University, Guangzhou, China;* [2]*Burning Rock Biotech, Guangzhou, China*

**Correspondence: yanh_liu@163.com*
[#]Contributed equally to this work.

Received May 27, 2024 / Accepted September 12, 2024

MYC-rearranged high-grade B-cell lymphoma (HGBCL) patients with concurrent *BCL2* rearrangements (HGBCL-*MYC/BCL2*) often have a poor prognosis with standard chemoimmunotherapy and may benefit from more intensified regimens. Conventional fluorescence *in situ* hybridization (FISH) is the gold standard for detecting rearrangements, but it has several limitations. This study compared DNA- and RNA-sequencing with FISH to detect clinically relevant rearrangements in HGBCL. Archived formalin-fixed, paraffin-embedded samples from 34 patients who underwent FISH testing were analyzed using targeted DNA- and RNA-sequencing. DNA- and RNA-sequencing identified six and five out of the 12 *MYC* rearrangements detected by FISH, 10 and 6 out of 10 FISH-detectable *BCL2* rearrangements, and 13 and 10 out of the 18 FISH-detectable *BCL6* rearrangements. When combining DNA- and RNA-sequencing (integrated NGS), the sensitivity for detecting *MYC*, *BCL2*, and *BCL6* rearrangements was 58.3%, 100%, and 73.7%, respectively. Both DNA- and RNA-sequencing detected the *EIF4A2::BCL6* fusion missed by FISH. FISH identified 12 HGBCL-*MYC/BCL2* out of 34 cases, while the integrated NGS strategy identified 7 cases, with 5 cases showing discordant results (41.7%). Additionally, patients with DLBCL/HGBCL-*MYC/BCL2* had significantly shorter overall survival than other patients. Our results suggest that an integrated NGS strategy should not replace FISH or be routinely used in the workup to detect the clinically relevant rearrangements in HGBCL. It may serve as a complement to FISH testing when FISH shows negative results.

Key words: next-generation sequencing; high-grade B-cell lymphoma; MYC; BCL2; BCL6

High-grade B-cell lymphoma (HGBCL) describes a group of highly aggressive and rapidly progressing lymphomas. In the 4th edition (2016) of the World Health Organization (WHO) classification, HGBCL is classified into two groups: HGBCL with *MYC* and *BCL2* and/or *BCL6* rearrangements ("double-hit" or "triple-hit", HGBCL-DH/TH), and HGBCL, not otherwise specified (NOS). With significant progress in the characterization of malignancies of the immune system, many new insights have been provided by genomic studies in recent years, and updates of the classification of HGBCL have been subsequently generated. The 5th edition (2022) of the WHO classification renames HGBCL-DH/TH to diffuse large B-cell lymphoma (DLBCL)/HGBCL with *MYC* and *BCL2* rearrangements (DLBCL/HGBCL-*MYC/BCL2*) [1]. However, the International Consensus Classification (ICC) of mature lymphoid neoplasms 2022 remains HGBCL-DH and defines it as comprising two groups: HGBCL with *MYC* and *BCL2* rearrangements (with or without *BCL6* rearrangement) (HGBCL-DH-*BCL2*) and a new provisional entity, HBGBL with *MYC* and *BCL6* rearrangements (HGBCL-DH-*BCL6*).

It has been reported that *MYC* gene rearranged in 5–14% of DLBCLs [2]. In approximately 60% of *MYC*-rearranged cases, the *MYC* gene is translocated to an immunoglobulin (IG) gene, with the heavy chain (*IGH*) gene being the most common partner. This translocation juxtaposes the *MYC* gene to the enhancer of the IG gene, leading to constitutive activation of MYC expression [3]. A large proportion

of *MYC*-rearranged HGBCLs harbor concurrent *BCL2* and or *BCL6* rearrangements [4]. Compared with NOS, DLBCL/HGBCL-*MYC/BCL2* are more aggressive. Those patients have a poor prognosis when treated with standard chemoimmunotherapy and may benefit from more intensified regimens [5, 6]. Therefore, identifying *MYC*, *BCL2*, and *BCL6* rearrangements in HGBCL is of vital clinical significance.

Fluorescence *in situ* hybridization (FISH) remains the gold standard for detecting rearrangements in lymphoma. Despite its wide utility in clinical practice, FISH has several limitations. Since it relies on good quality of cell morphology, necrosis, apoptosis, and crush artifacts may impact reliable interpretation. The analyzing process is performed largely in a manual manner, which is error-prone and labor-intensive [7, 8]. Moreover, rearrangement assessment may be equivocal under the circumstance of complex patterns of fluorescent signals caused by uncommon breakpoints, polysomy, or deletions [9]. *MYC/IGH* dual fusion FISH (D-FISH) fails to identify translocation with non-canonical partner and has been reported to result in a high false positive rate of 22.1%. The routinely used break-apart FISH also confers a false positive of at least 4%, which can be mitigated by D-FISH [10]. Recently, studies have demonstrated that next-generation sequencing (NGS)-based approaches can identify *MYC* and *BCL2* rearranged events that are cryptic to both FISH approaches [11, 12], suggestive of the feasibility of improving the sensitivity of detecting DLBCL/HGBCL-*MYC/BCL2* cases by incorporating multiple test platforms.

NGS-based techniques, encompassing both DNA- and RNA-sequencing, have increasingly been utilized to detect gene rearrangements in cancer management, including hematologic malignancies [13]. However, current studies that, in parallel, compare the performance of detecting DLBCL/HGBCL-*MYC/BCL2* between FISH and NGS approaches remain limited. In the present study, we conducted a comparative study to comprehensively investigate the results of *MYC*, *BCL2*, and *BCL6* rearrangements identified by FISH, targeted DNA-, and RNA-sequencing in HGBCLs.

Patients and methods

Patients and study design. Patients with DLBCL/HGBCL who met the inclusion criteria below were retrospectively included from Guangdong Provincial People's Hospital between 2019 and 2020: 1) older than 18 years; 2) having sufficient archived formalin-fixed, paraffin-embedded (FFPE) samples for FISH assessment, targeted DNA-sequencing, and RNA-sequencing. Clinical and demographic characteristics were obtained from medical records. Additionally, the results of FISH and immunohistochemistry (IHC) testing for these genes were also retrieved for comparison. This study has been approved by the Ethics Committee of Guangdong Provincial People's Hospital (KY-Z-2020-664-02). The flow chart of the study is summarized in Supplementary Figure S1.

Fluorescence *in situ* hybridization. FISH was conducted on 4 μm FFPE tissue sections according to the instructions of the manufacturer for each probe (Vysis, Abbott Molecular IL, USA). The following probes were used: *MYC* break-apart probe, *BCL2* break-apart probe, *BCL6* break-apart probe, and dual fusion probes for *IGH*::*MYC*. The schematic diagram for the captured regions of the four probes is provided in Supplementary Figure S2. A total of 100 cells were read in areas of interest for each probe, and rearrangement was considered positive if intended signals were observed in more than 10% of cells.

Immunohistochemical testing. IHC testing was performed to determine the cell of origin according to the Hans algorithm as follows: CD10+ or CD10–BCL6+MUM1– for GCB, and CD10–BCL6–MUM1+ or CD10–BCL6+MUM1+ or CD10–BCL6–MUM1– for non-GCB [14]. IHC was also performed using antibodies against MYC and BCL2 (Leica S2) as defined by protein expression of the *BCL2* gene in at least 50% of all lymphoma cells and protein expression of the *MYC* gene in at least 40% of all lymphoma cells as per WHO criteria [2].

Targeted DNA-sequencing. DNA was extracted from the FFPE tissue sample using the QIAamp DNA FFPE tissue kit (Qiagen, Hilden, Germany) and subjected to library preparation using a panel including 112 genes related to lymphoma (Burning Rock Biotech, Guangzhou, China) (Supplementary Table S1) as described previously [15]. Indexed DNA libraries were sequenced using the Nextseq500 sequencer (Illumina, Inc., Hayward, USA) with a depth of 1,000× per sample. Data analyses, including variants calling and interpretation, copy number variation, were carried out using standardized pipelines based on the methods described previously [16]. Structural rearrangement was analyzed using an in-house algorithm markSV (Burning Rock Biotech, Guangzhou, China), which integrates split-read and paired-end analysis and is suitable for identifying deletions, tandem duplication events, inversions, and translocations [17]. The breakpoints of MYC, BCL2, and BCL6 covered by the probes of the DNA panel are demonstrated in Supplementary Table S2.

RNA-sequencing. RNA was extracted from an FFPE tissue sample using an AllPrep DNA/RNA FFPE Kit (Qiagen, Hilden, Germany). Strand-specific cDNA synthesis, dA-tailing, ligation of unique molecular identifier adaptor, and PCR amplification were subsequently performed and followed by hybridization using a panel with customized capture probe baits, which spans full transcripts of genes commonly involved in cancer genomic rearrangements. The prepared libraries were sequenced, and sequencing data was analyzed as previously described [17]. The clean reads were aligned and called for gene rearrangements using STAR (2.7.3a). The raw read counts were utilized to identify differentially expressed genes (DEG) between DLBCL/HGBCL-*MYC/BCL2* and DLBCL, NOS patients by R package"DEseq2". The up- and downregulated genes were defined with a $p<0.05$ and the log2(fold change (FC)) >1 and <–1, respectively.

Statistical analysis. Patient characteristics were summarized with descriptive statistics. The sensitivity, specificity, and concordance of NGS approaches were calculated using the FISH as the gold standard. The sensitivity was defined as the ratio of the number of true positive cases to the sum of true positive and false negative cases. The specificity was defined as the ratio of the number of true negative cases to the sum of true negative and false positive cases. The concordance was defined as the proportion of subjects with true positive and true negative. Differences between groups were compared using Fisher's exact test or chi-square test for categorical data and the Wilcoxon signed-rank test for continuous data, as applicable. A p-value <0.05 was considered statistically significant. All data were analyzed using R software. Kaplan-Meier curves and Log-rank test were performed to delineate the difference of survival outcome between groups. The online DAVID software (https://david.ncifcrf.gov/) was used for the Kyoto Encyclopedia of Genes and Genomes (KEGG) pathway enrichment based on identified DEGs.

Table 1. Characteristics of patients.

Characteristic	Overall (n=34)
Sex, No. (%)	
Female	20 (58.8)
Male	14 (41.2)
Age, years	
Median	62.50
Range	24-81
Specimen, No. (%)	
Needle biopsy	6 (17.6)
Surgical	28 (82.4)
Hans subtype, No. (%)	
GCB	18 (52.9)
Non-GCB	16 (47.1)
Co-expressor, No. (%)	
No	14 (41.2)
Yes	20 (58.8)

Abbreviations: No-number; GCB-germinal-center B-cell like; NGCB-non-germinal-center B-cell like

Results

Clinical characteristics of patients. A total of 34 patients were included in this study, providing eligible DNA- and RNA-sequencing data from their FFPE samples for subsequent analyses. The median age of the cohort was 62 years, with 58.8% being female. The majority (82.4%) of patients provided surgical samples, and 6 patients provided needle biopsy samples. Eighteen (52.9%) patients were identified with the GCB subtype, and 20 were recognized as co-expressors (Table 1).

Molecular alterations in DLBCL patients. DNA profiling studies identified alterations in *BCL6* (44%), *PIM1*(41%), *BCL2* (38%), and *KMT2D* (29%) (Supplementary Figure S3) were the most common alterations. *MYC* alterations were detected in 26% of patients (Supplementary Figure S3). RNA-sequencing detected rearrangements in 18 patients, including 5 with *MYC* rearrangements, 6 with *BCL2* rearrangements, 11 with *BCL6* rearrangements, 1 with an intergenic (*IGHEP1, IGHG1*)::*KDM2B* rearrangement, 1 with a *KDM2B*::*IGHE* rearrangement, and 1 with a *ZNF41*::*SYK* rearrangement. Eight out of 18 patients harbored more than one rearrangement detected by RNA-sequencing.

The performance of NGS in detecting rearrangements. FISH identified *MYC* rearrangements in 12 out of 34 patients (35.3%). Among the 12 *MYC*-rearranged cases, DNA-sequencing detected *MYC* rearrangements in 6, resulting in a sensitivity of 50% and a concordance of 82.4% (Figure 1A, Supplementary Figure S4A). On the other hand, RNA-sequencing only identified 5 out of the 12 FISH-detectable *MYC* rearrangements, conferring a sensitivity of 41.7% and a concordance of 79.4% (Supplementary Figure S4A). Of note, RNA-sequencing failed to identify 2 rearrangements that were detected by DNA-sequencing (p001 and p009) but recognized 1 event missed by DNA-sequencing (p004) (Figure 1A, Supplementary Table S2). Representative images with concordant FISH and integrated NGS on *MYC* rearrangement (p007) are shown in Supplementary Figure S5. Integrating both DNA- and RNA-sequencing

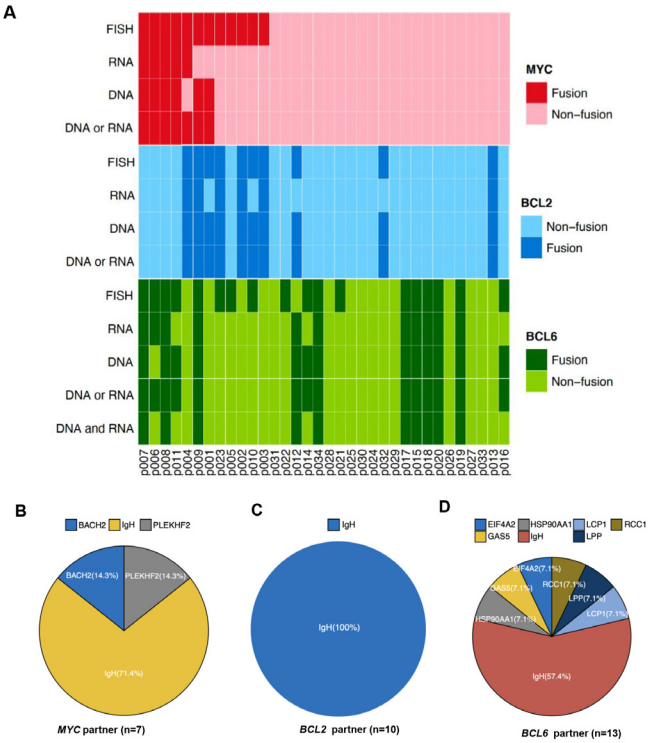

Figure 1. Detection of *MYC/BCL2* rearrangements using different methods. A) Results for FISH, DNA-, and RNA-sequencing in detecting *MYC* and *BCL2* rearrangements. Distribution of partners identified for *MYC* (B) and *BCL2* (C) using DNA- or RNA-sequencing. Abbreviation: FISH-fluorescence *in situ* hybridization

(integrated NGS) results improved the sensitivity to 58.3% for detecting *MYC* rearrangements, yielding a concordance of 85.3% compared with FISH (Figure 2A). As illustrated in Figure 1B, 74.1% of *MYC* rearrangements (identified by NGS) had an *IGH* partner (n=5), 1 was fused with *PLEKHF2*, and 1 with *BACH2*. Representative images with discordant FISH and integrated NGS on *MYC* rearrangements are shown in Figure 3, which indicated that *MYC* fusion in p003 was detectable by FISH and IHC rather than DNA-/RNA-sequencing.

Regarding *BCL2* rearrangement, FISH identified 10 events from 34 patients (29.4%), 100% of which were detectable by DNA-sequencing (Figure 1A). In contrast, RNA-sequencing missed 4 events conferring a sensitivity of 60% (Supplementary Figure S4B). DNA-sequencing achieved a concordance of 100% compared with FISH, while RNA-sequencing showed a concordance of 88.2%. All the 10 *BCL2* rearrangements were detected with an *IGH* partner (Figure 1C). The 4 RNA-seq false negative cases showed intergenic breakpoints (p001, p010, p12, and p023, Supplementary Table S3), which might contribute to the production of wild-type *BCL2* transcripts that are undetectable by RNA-sequencing. Integrating DNA- and RNA-sequencing resulted in a sensitivity of 100% and a concordance of 100% in detecting *BCL2* rearrangements (Figure 2B). Representative images with concordant FISH and integrated NGS on *BCL2* rearrangement are shown in Supplementary Figure S6 (p023).

BCL6 rearrangements were identified in 18 out of 34 patients (35.3%) using FISH. Of the 18 FISH-detectable rearrangements, 13 (72.2%) were identified by DNA-sequencing and 10 (55.6%) by RNA-sequencing (Figure 1A, Supplementary Figure S4C). Notably, both DNA- and RNA-sequencing detected one *BCL6* rearrangement (*EIF4A2-BCL6*) that FISH failed to detect (p012, Table 2, Supplementary Table S3). Collectively, DNA- and RNA-sequencing showed a concordance of 79.4% and 73.5% with FISH, respectively. Of the 14 rearrangements detected by NGS, eight (57.4%) had an *IGH* partner. Other partners were each seen in one case, including *EIF4A2*, *RCC1*, *GAS5*, *LPP*, *LCP1,* and *HSP90AA1* (Figure 1D). Incorporating both DNA- and RNA-sequencing demonstrated a concordance of 82.4% with FISH and a sensitivity of 73.7% in detecting *BCL6* rearrangements (Figure 2C). Combining DNA- and RNA-sequencing (integrated NGS) resulted in a sensitivity of 73.7% for detecting *BCL6* rearrangements. Notably, both DNA- and RNA-sequencing detected the *EIF4A2::BCL6* fusion that was missed by FISH (Supplementary Figure S7).

These data showed integrated DNA- and RNA-sequencing improved the sensitivity of detecting *MYC/BCL6* rearrangements compared with DNA- or RNA-sequencing alone. In addition, both DNA and RNA-sequencing detected a *BCL6* rearrangement missed by FISH, indicating that integrated DNA- and RNA-sequencing could complement FISH testing in detecting rearrangement events of DLBCLs/HGBCLs.

A

	FISH		
DNA/RNA-sequencing	*MYC+*	*MYC-*	
MYC+	7	0	Accuracy=85.3%
MYC-	5	22	
	Sensitivity=58.3%	Specificity=100%	

B

	FISH		
DNA/RNA-sequencing	*BCL2+*	*BCL2-*	
BCL2+	10	0	Accuracy=100%
BCL2-	0	24	
	Sensitivity=100%	Specificity=100%	

C

	FISH		
DNA/RNA-sequencing	*BCL2+*	*BCL2-*	
BCL6+	13	1	Accuracy=82.4%
BCL6-	5	15	
	Sensitivity=73.7%	Specificity=100%	

Figure 2. Performance of integrative DNA- and RNA- sequencing in detecting *MYC* (A) and *BCL2* rearrangements (B). Abbreviations: DLBCL-diffuse large B-cell lymphoma; FISH-fluorescence *in situ* hybridization

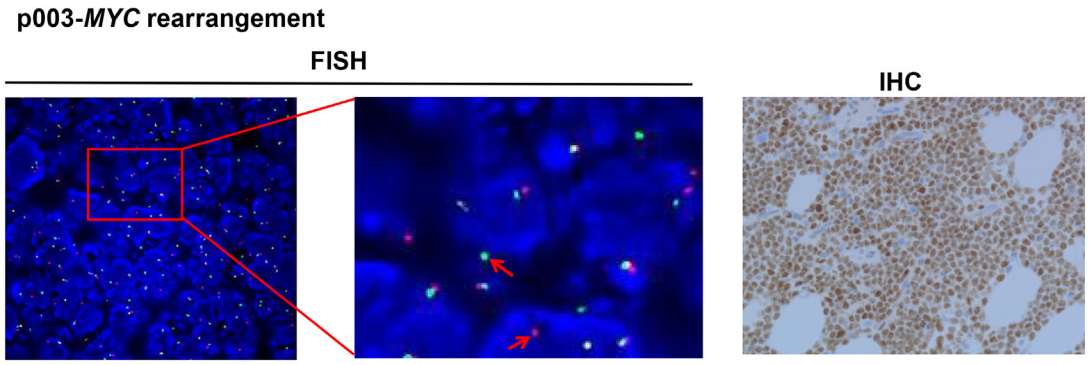

Figure 3. Representative images with discordant FISH and integrated DNA- and RNA-sequencing in detecting *MYC* rearrangements. *MYC* fusion in p003 was detectable by FISH and IHC but not by DNA-/RNA-sequencing. Red arrows and brown color indicate the presence of *MYC* fusion and MYC expression detected by FISH and IHC (×400), respectively. Abbreviations: FISH-fluorescence *in situ* hybridization; IHC-immunohistochemistry

The performance of NGS in identifying certain subtypes of patients. HGBCL-*MYC/BCL2* represents a subset of HGBCLs without a standard approach to treatment. Applying criteria from the 5th edition of the WHO classification, 7 (p002, p003, p010, p023, p001, p004, and p009) cases classified as DLBCL/HGBCL-*MYC/BCL2* were identified by FISH, while 3 cases were identified by integrated NGS with 4 cases showing discordant results (Table 2, Supplementary Table S3). Based on the ICC of mature lymphoid neoplasms, 7 (p001, p002, p003, p004, p009, p010, p023) and 5 (p005, p006, p007, p008, p011) patients were respectively identified as HGBCL-DH-*BCL2* and HGBL-DH-*BCL6* by FISH, while the numbers were 3 (p001, p004, p009) and 4 (p006, p007, p008, p011) by integrated NGS.

Comparison of molecular alterations/survival outcome between HGBCL-*MYC/BCL2* and DLBCL, NOS patients. We also compared the genomic profile between DLBCL/HGBCL-*MYC/BCL2* (as per the 2022 WHO classification) and other patients. DLBCL/HGBCL-*MYC/BCL2* group harbored a higher median count of alterations (16 vs. 7, p=0.031, Figure 4A). In addition, more patients who harbored alterations in the MAPK pathway (71.4% vs. 22.2%, p=0.024, Figure 4B) were observed in the DLBCL/HGBCL-*MYC/BCL2* group. According to RNA-sequencing, a total of 136 DEGs were identified in DLBCL/HGBCL-*MYC/BCL2* compared with DLBCL, NOS patients (Figure 4C). These DEGs were significantly enriched in transcriptional misregulation in cancer, pathways in cancer, cell adhesion molecules, and Pl3K-Akt signaling pathway (Figure 4D). Next, whether DLBCL/HGBCL-*MYC/BCL2* patients had a worse prognosis than other patients was explored. In this cohort, 33 out of 34 DLBCL patients had available survival data, including 7 DLBCL/HGBCL-*MYC/BCL2* and 26 DLBCL, NOS patients as per FISH detection. Kaplan-Meier curves showed that DLBCL/HGBCL-*MYC/BCL2* patients had an unfavorable OS compared with DLBCL, NOS patients (p=0.096, not reached [NR] vs. NR, Figure 4E).

Table 2. Discordant FISH and NGS results in detecting *MYC*, *BCL2*, and *BCL6* rearrangements.

No. of patient	Rearrangement (FISH)	Rearrangement (NGS)
p002	*MYC* and *BCL2*	*BCL2*
p003	*MYC* and *BCL2*	*BCL2*
p005	*MYC* and *BCL6*	ND
p010	*MYC*, *BCL2* and *BCL6*	*BCL2*
p012	*BCL2*	*BCL2 and BCL6*
p023	*MYC*, *BCL2* and *BCL6*	*BCL2*

Abbreviations: No- number; FISH-Fluorescence *in situ* hybridization; NGS-integrated DNA- and RNA sequencing; ND-not detected

Applying criteria from the ICC of mature lymphoid neoplasms, 12 HGBCL-DH (including 7 HGBCL-DH-*BCL2* and 5 -*BCL6* patients) and 22 DLBCL, NOS patients as per FISH detection were identified. Among the 12 HGBCL-DH patients, 11 had available survival data. Kaplan-Meier curves showed that HGBCL-DH patients had a significantly shorter OS than DLBCL and NOS patients (p=0.0087, NR vs. NR, Figure 5A). We then categorized HGBCL into three groups according to the ICC classification: HGBCL-NOS, HGBCL-DH-BCL2, and HGBCL-DH-BCL6. Both HGBCL-DH-BCL2 and HGBCL-DH-BCL6 patients had or tended to have a significantly worse OS than DLBCL, NOS (HGBCL-DH-BCL2, p=0.051, HR, 5.97; 95% CI, 0.99–35.87; HGBCL-DH-BCL6, p=0.035, HR, 8.36; 95% CI, 1.16–60.11; Figure 5B).

Discussion

In this work, we compared the detection of *MYC/BCL2/BCL6* rearrangements among FISH, DNA- and RNA-sequencing approaches. Our results revealed that DNA-sequencing generally exhibited a higher sensitivity than RNA-sequencing in detecting *MYC/BCL2/BCL6* rearrangements, which was attributable to the fact that these rearrangements often occur in non-coding regions (such

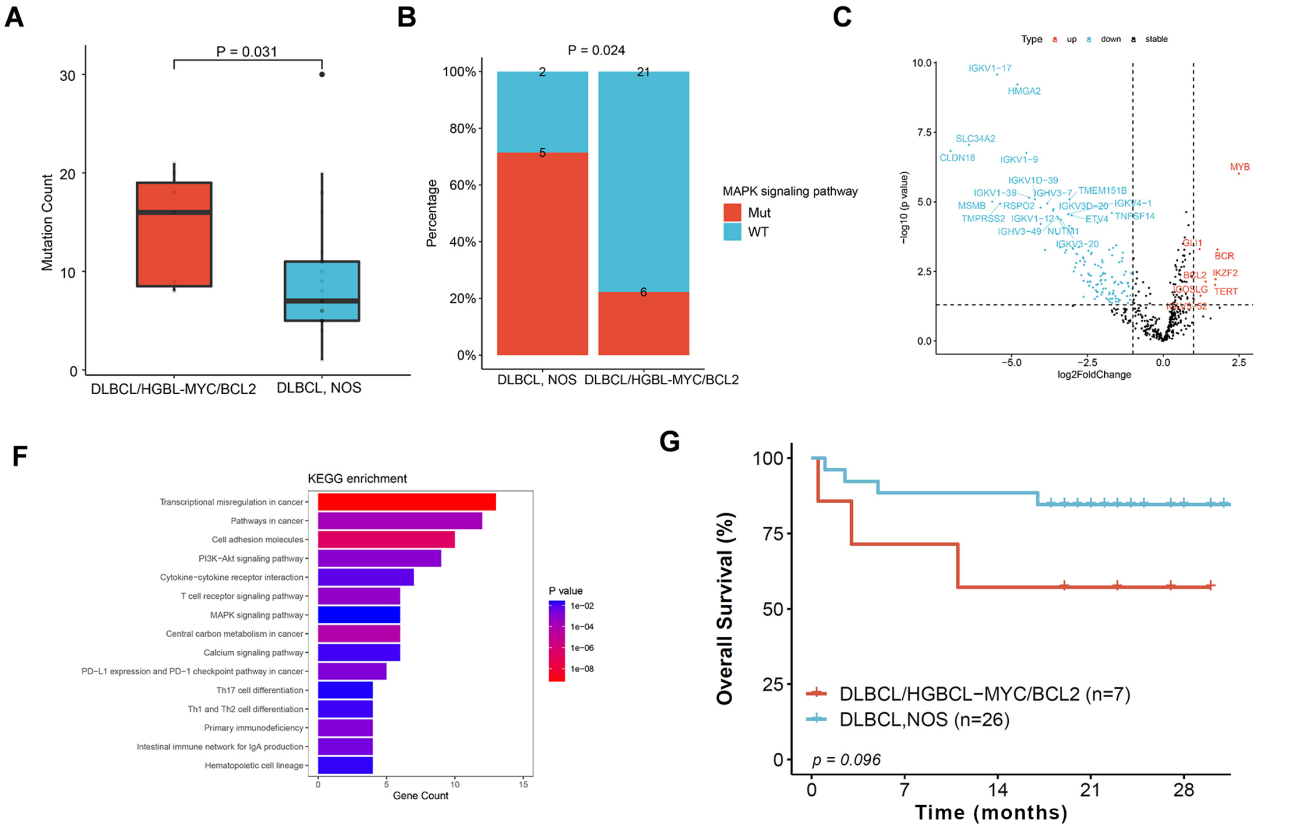

Figure 4. Molecular alterations in DLBCL/HGBCL-*MYC/BCL*. A comparison of mutation count (A) and alterations in MAPK signaling pathway (B) between DLBCL/HGBCL-*MYC/BCL2* and DLBLC, NOS patients. DEGs (C) and enriched signaling pathways from DEGs (D) in DLBCL/HGBCL-*MYC/BCL2* vs. DLBLC, NOS patients based on RNA-sequencing results. E) Kaplan-Meier curves by FISH-based molecular subtype. Abbreviations: DLBCL/HGBCL-*MYC/BCL2*-diffuse large B-cell lymphoma/high-grade B-cell lymphoma with *MYC* and *BCL2* rearrangements; NOS-not otherwise specified; DEG-differentially expressed genes

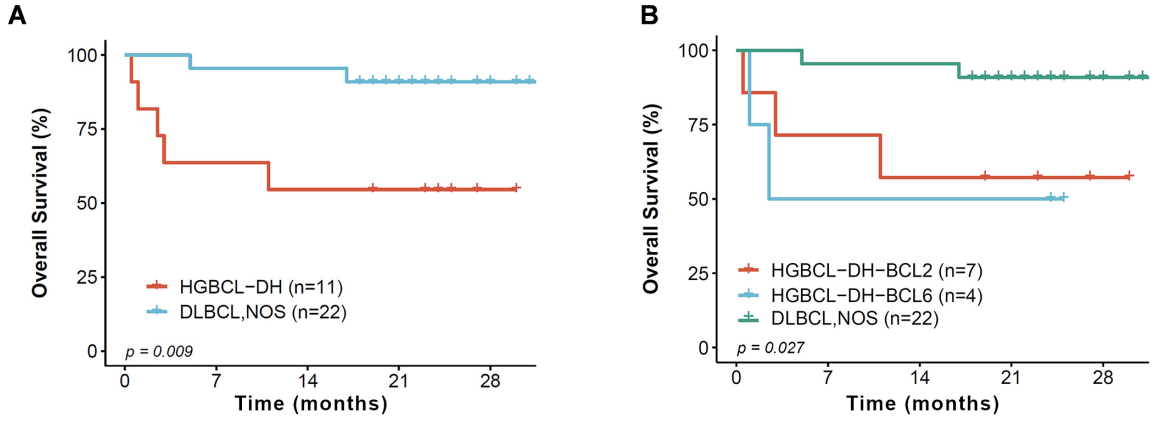

Figure 5. Difference in overall survival between HGBCL-DH and DLBCL, NOS patients. A) Kaplan-Meier curves comparing overall survival between HGBCL-DH and DLBCL, NOS patients; B) Kaplan-Meier curves comparing overall survival between HGBCL-DH-BCL2, HGBCL-DH-BCL6 and DLBCL, NOS patients. Abbreviations: HGBCL-high-grade B-cell lymphoma; DH-double hit; NOS-not other specified; ICC-International Consensus Classification

as enhancer sequencing of immunoglobulin genes) and do not form RNA-sequencing-detectable fusion products. Similarly, Wang et al. compared the RNA-sequencing with FISH and found that RNA-sequencing had relatively low sensitivities, only detecting 1/7 *MYC* (14%) and 3/8 *BCL2* (38%) rearrangements identified by FISH [18]. Five *MYC* and 6 *BCL6* rearrangements were missed by both DNA- and RNA-sequencing, which might be due to the tumor

heterogeneity that only a few of the tumor cells harbor these rearrangements, leading to low frequency undetectable by NGS. An exception was noted in one case, where a non-canonical *BACH2::MYC* fusion was only detected by RNA- but not DNA-sequencing. Besides tumor heterogeneity, another cause of detection failure might be breakpoints occurring at non-coding regions not covered in the panel used in this study.

Integrating DNA- and RNA-sequencing demonstrates improved sensitivities (58.3% for *MYC* and 100% for *BCL2*), yet remains unsatisfactory compared with FISH. This might be explained by the fact that DNA-sequencing relies on detecting unambiguous fusion-reads to identify rearrangements; however, non-unique sequencing flanking the breakpoint is the common scenario for oncogene rearrangements (typically with immunoglobulin and T-cell receptor genes as partners) in malignant lymphoma [19]. Previous studies have demonstrated that integrated NGS was superior to FISH in the detection of *IGH::MYC* rearrangements but was inferior in the detection of non-*IGH::MYC* rearrangements [12, 20]. Unfortunately, in our study, the *MYC/IGH* dual fusion FISH probe was not routinely used for *MYC*-positive samples identified by break-apart FISH; thus, we could not identify partners of the *MYC* rearrangements missed by NGS. The performance of integrated NGS in detecting *IGH::MYC* and non-*IGH::MYC* rearrangements were not explored.

Although FISH is used to detect rearrangement events in routine clinical practice, it has certain limitations. For example, FISH analysis is typically limited to assessing a single or a few fusion events at a time, making it challenging to simultaneously evaluate multiple fusion genes or detect novel fusion events. Additionally, FISH results can be subjective and may vary between observers, especially for complex FISH signal patterns, requiring experienced pathologists for accurate interpretation [7, 21]. In this study, the NGS strategy detected an *EIF4A2*::*BCL6* rearrangement that was missed by FISH. The *EIF4A2* gene is located on chromosome 3q27, close to *BCL6,* in a tail-to-tail orientation. *EIF4A2*::*BCL6* rearrangement is produced by a paracentric inversion cryptic to FISH detection [18, 22]. The detection failure of the rearrangement by FISH might be due to the number of bases between the breakpoint and fusion site being less than the minimum threshold detected by FISH, potentially resulting in false negatives. These data suggest the necessity of NGS for HGBCL samples identified with FISH-negative results, and NGS could complement FISH testing in detecting rearrangements from DLBCLs.

In this work, 5 *MYC* fused with *IGH* events, 10 *BCL2* fused with *IGH* events, and 6 *BCL6* fused with *IGH* events were detected by DNA-sequencing, while 1 *MYC* fused with *IGH* event (*IGHG1::MYC*) and 4 *BCL2* fused with *IGH* events (*IGHD3-10*::intergenic(*PHLPP1,BCL2*), intergenic(*PHLPP 1,BCL2*)::*IGHJ6*, intergenic(*PHLPP1, BCL2*)::*IGHJ6*, and intergenic(*PHLPP1,BCL2*)::*IGHJ2*), and 1 *BCL6* fused with *IGH* event (*IGHA1::BCL6*) were missed by RNA-sequencing. Of these, 4 *BCL2* rearrangements are undetectable by RNA-sequencing, with the breakpoints occurring at non-coding regions. The *IGHG1::MYC* and *IGHA1::BCL6* rearrangements missed by RNA-sequencing might be attributed to the production of chimeric products, which suggests the importance of filtering optimization for *IGH* gene fusion events. Further study is warranted to optimize the bioinformatics analysis workflows for detecting gene fusions in HGBCL.

FISH-based DLBCL/HGBCL-*MYC/BCL2* patients were observed to have a significantly shorter OS than DLBCL, NOS patients, which kept in line with previous studies indicating that DLBLCs with concurrent *MYC* and *BCL2* and/or *BCL6* arrangements are more aggressive than DLBCL, NOS patients [5, 6]. These data suggest the need to identify DLBCL/HGBCL-*MYC/BCL2* patients who might benefit from intensified chemotherapy regimens or should enroll in clinical trials investigating novel regimens.

There are some limitations in this work. First, since the *IGH-MYC* rearrangements were not distinguished from non-*IGH-MYC* rearrangements with our FISH analysis, the performance of the integrated NGS strategy in detecting *IGH-MYC* rearrangements was not delineated. In DLBCL, non-*IGH MYC-R* typically involved non-IG loci such as *PAX5*, while non-IGH partners of *MYC* rearrangements in HGBCL-DH-*BCL2* tumors included frequently *BCL6, PAX5, IRAG2*, and *RFTN*1 [23]. *IGH-MYC* rearrangements consistently occur centromeric to *MYC*, focused in the 5' flank, 5' untranslated region (UTR), and intron 1 of *MYC,* whereas non-IGH rearrangements are consistently telomeric, occurring up to 600 kb downstream of the *MYC* gene. Due to the probe design, the DNA panel used in the current study can cover the most common breakpoints of *MYC*, including 3 kb upstream, exon1, intron 1, exon 2, and exon 3 of *MYC*, but not all potential *MYC* rearrangement sites. The whole transcriptomic sequencing we used may capture potential transcript fusion events missed by the DNA panel but still may not be sensitive enough to compensate for the lack of breadth of the DNAseq capture. Second, the sample size of the cohort was relatively small, so we were unable to further explore the differences between HGBCL-DH-*BCL2* and HGBCL-DH-*BCL6*. The performance of integrated NGS in identifying clinically relevant rearrangements needs to be investigated in a large cohort of patients.

In conclusion, although integrated NGS sequencing could identify more *MYC* rearrangements than DNA- or RNA-sequencing alone, its sensitivity in detecting *MYC* rearrangements was unsatisfactory. Our study suggests that gene rearrangements could be better detected by FISH combined with integrated NGS testing rather than either method alone, and DLBCL/HGBCL patients might benefit from the combined testing in clinical practice.

Supplementary information is available in the online version of the paper.

Acknowledgments: This work is supported by the Guangdong Medical Science and Technology Research Fund (B2021187).

References

[1] ALAGGIO R, AMADOR C, ANAGNOSTOPOULOS I, ATTYGALLE AD, ARAUJO IBO et al. The 5th edition of the World Health Organization Classification of Haematolymphoid Tumours: Lymphoid Neoplasms. Leukemia 2022; 36: 1720–1748. https://doi.org/10.1038/s41375-022-01620-2

[2] SWERDLOW SH, CAMPO E, PILERI SA, HARRIS NL, STEIN H et al. The 2016 revision of the World Health Organization classification of lymphoid neoplasms. Blood 2016; 127: 2375–2390. https://doi.org/10.1182/blood-2016-01-643569

[3] KARUBE K, CAMPO E. MYC alterations in diffuse large B-cell lymphomas. Sem Hematol 2015; 52: 97–106. https://doi.org/10.1053/j.seminhematol.2015.01.009

[4] DODERO A, GUIDETTI A, MARINO F, TUCCI A, BARRETTA F et al. Dose-adjusted EPOCH and rituximab for the treatment of double expressor and double-hit diffuse large B-cell lymphoma: impact of TP53 mutations on clinical outcome. Haematologica 2022; 107: 1153–1162. https://doi.org/10.3324/haematol.2021.278638

[5] FRIEDBERG JW. How I treat double-hit lymphoma. Blood 2017; 130: 590–596. https://doi.org/10.1182/blood-2017-04-737320

[6] SESQUES P, JOHNSON NA. Approach to the diagnosis and treatment of high-grade B-cell lymphomas with MYC and BCL2 and/or BCL6 rearrangements. Blood 2017; 129: 280–288. https://doi.org/10.1182/blood-2016-02-636316

[7] BAILEY NG, ELENITOBA-JOHNSON KSJ. Impact of Genetics on Mature Lymphoid Leukemias and Lymphomas. Cold Spring Harb Perspect Med 2020; 10: a035444. https://doi.org/10.1101/cshperspect.a035444

[8] GOZZETTI A, LE BEAU MM. Fluorescence in situ hybridization: uses and limitations. Sem Hematol 2000; 37: 320–333. https://doi.org/10.1016/s0037-1963(00)90013-1

[9] ALLAHYAR A, PIETERSE M, SWENNENHUIS J, LOS-DE VRIES GT, YILMAZ M et al. Robust detection of translocations in lymphoma FFPE samples using targeted locus capture-based sequencing. Nat Commun 2021; 12: 3361. https://doi.org/10.1038/s41467-021-23695-8

[10] KING RL, MCPHAIL ED, MEYER RG, VASMATZIS G, PEARCE K et al. False-negative rates for MYC fluorescence in situ hybridization probes in B-cell neoplasms. Haematologica 2019; 104: e248–e51. https://doi.org/10.3324/haematol.2018.207290

[11] HILTON LK, TANG J, BEN-NERIAH S, ALCAIDE M, JIANG A et al. The double-hit signature identifies double-hit diffuse large B-cell lymphoma with genetic events cryptic to FISH. Blood 2019; 134: 1528–1532. https://doi.org/10.1182/blood.2019002600

[12] CASSIDY DP, CHAPMAN JR, LOPEZ R, WHITE K, FAN YS et al. Comparison Between Integrated Genomic DNA/RNA Profiling and Fluorescence In Situ Hybridization in the Detection of MYC, BCL-2, and BCL-6 Gene Rearrangements in Large B-Cell Lymphomas. Am J Clin Pathol 2020; 153: 353–359. https://doi.org/10.1093/ajcp/aqz172

[13] HE J, ABDEL-WAHAB O, NAHAS MK, WANG K, RAMPAL RK et al. Integrated genomic DNA/RNA profiling of hematologic malignancies in the clinical setting. Blood 2016; 127: 3004–3014. https://doi.org/10.1182/blood-2015-08-664649

[14] SEHN LH, SALLES G. Diffuse Large B-Cell Lymphoma. N Engl J Med 2021; 384: 842–858. https://doi.org/10.1056/NEJMra2027612

[15] JIANG S, QIN Y, JIANG H, LIU B, SHI J et al. Molecular profiling of Chinese R-CHOP treated DLBCL patients: Identifying a high-risk subgroup. Int J Cancer 2020; 147: 2611–2620. https://doi.org/10.1002/ijc.33049

[16] WANG M, CHEN X, DAI Y, WU D, LIU F et al. Concordance Study of a 520-Gene Next-Generation Sequencing-Based Genomic Profiling Assay of Tissue and Plasma Samples. Mol Diagn Ther 2022; 26: 309–322. https://doi.org/10.1007/s40291-022-00579-1

[17] XIANG C, GUO L, ZHAO R, TENG H, WANG Y et al. Identification and Validation of Noncanonical RET Fusions in Non-Small-Cell Lung Cancer through DNA and RNA Sequencing. J Mol Diagn 2022; 24: 374–385. https://doi.org/10.1016/j.jmoldx.2021.12.004

[18] WANG X, JOHNSON V, JOHNSON L, COOK JR. RNA-Based next generation sequencing complements but does not replace fluorescence in situ hybridization studies for the classification of aggressive B-Cell lymphomas. Cancer Genet 2021; 252–253: 43–47. https://doi.org/10.1016/j.cancergen.2020.12.004

[19] HASTY P, MONTAGNA C. Chromosomal Rearrangements in Cancer: Detection and potential causal mechanisms. Mol Cell Oncol 2014; 1: e29904. https://doi.org/10.4161/mco.29904

[20] DE LIMA GUIDO LP, CHAPMAN J, CASSIDY DP. Integrated Genomic DNA/RNA Profiling vs Fluorescence in Situ Hybridization in the Detection of MYC and BCL2 (and BCL6) Rearrangements in Large B-Cell Lymphomas: Updates Amid the New WHO Classification of Lymphoid Neoplasms. Am J Clin Pathol 2023; 160: 41–48. https://doi.org/10.1093/ajcp/aqad006

[21] PISAPIA P, PEPE F, SGARIGLIA R, NACCHIO M, RUSSO G et al. Methods for actionable gene fusion detection in lung cancer: now and in the future. Pharmacogenomics 2021; 22: 833–847. https://doi.org/10.2217/pgs-2021-0048

[22] RUMINY P, JARDIN F, PICQUENOT JM, PENTHER D, PARMENTIER F et al. Promoter Shuffling by Sequential Genomic Rearrangements in Follicular Lymphoma Reveals an Ongoing Genomic Instability at the BCL6 Locus. Blood 2006; 108: 2074. https://doi.org/10.1182/blood.V108.11.2074.2074

[23] HILTON LK, COLLINGE B, BEN-NERIAH S, ALDUAIJ W, SHAALAN H et al. Motive and opportunity: MYC rearrangements in high-grade B-cell lymphoma with MYC and BCL2 rearrangements (an LLMPP study). Blood 2024; 144: 525–540. https://doi.org/10.1182/blood.2024024251

https://doi.org/10.4149/neo_2024_240527N236

Comparative investigation among fluorescence in situ hybridization, DNA- and RNA-sequencing on detecting MYC, BCL2, and BCL6 rearrangements in high-grade B-cell lymphomas

Fen ZHANG[1,#], Qian CUI[1,#], Haiwei DU[2], Xinze LV[2], Ting HOU[2], Yu CHEN[1], Jie CHEN[1], Jian LIU[1], Jinhai YAN[1], Yanhui LIU[1,*]

Supplementary Information

Supplementary Table S1. List of the 112 genes included in the DNA-sequencing panel.

ALK	*BCL2*	*BCL6*	*MYC*	*BIRC3*	*CD28*	*CTLA4*	*ITK*	*SYK*	*IGHD*	*IGHJ*
AIM1	APC	ARID1A	ARID1B	ARID2	ASXL3	ATG5	ATM	B2M	BCOR	BCORL1
BRAF	BTK	CARD11	CCND1	CCND2	CCND3	CD58	CD79A	CD79B	CDKN2A	CDKN2B
CHD8	CIITA	CREBBP	CTNNB1	CXCR4	DDX3X	DNMT3A	DNMT3B	DTX1	DUSP22	EP300
EZH2	FAS	FOXO1	FOXO3	FYN	GATA3	GNA13	ID3	IDH2	IRF4	ITPKB
JAK1	JAK3	KDM6A	KIR2DL4	KIR3DL2	KIT	KLHL6	KLRC1	KLRC2	KLRK1	KMT2A
KMT2C	KMT2D	KRAS	MAP2K1	MAP3K14	MEF2B	MET	MFHAS1	MGA	MTOR	MYD88
NF1	NOTCH1	NOTCH2	NRAS	PDGFRA	PIK3CA	PIM1	PRDM1	PTEN	RHOA	SETD2
SF3B1	SGK1	SOCS1	SPEN	SPI1	STAT3	STAT5B	STAT6	STK11	TBX21	TCF3
TET2	TNFAIP3	TNFRSF14	TP53	TP63	TP73	TRAF2	TRAF3	TSC1	TSC2	WHSC1
XPO1	ZAP70									

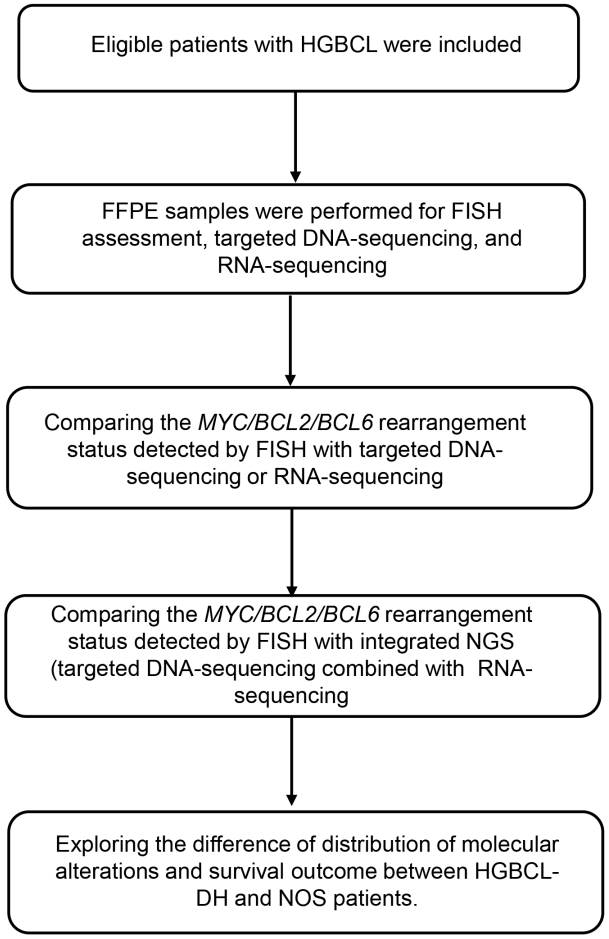

Supplementary Figure S1. Flow chart of the study. Abbreviations: HGBCL-high-grade B-cell lymphoma; DH-double hit; NOS-not other specified; NGS-next-generation sequencing; FFPE-formalin-fixed, paraffin-embedded

Supplementary Table S2

Gene	Chr	Start	End	Location (exon/intron)
MYC	8	128745443	128751315	intergenic, exon 1, intron 1, exon 2
MYC	8	128752591	128753254	exon 3
BCL2	18	60760528	60796042	exon 2
BCL2	18	60985231	60985949	intergenic, exon 1
BCL6	3	187442678	187442916	exon 9
BCL6	3	187443236	187443467	exon 8
BCL6	3	187460647	187463565	exon 1, intron 1

Supplementary Table S3. The FISH, DNA-sequencing, RNA-sequencing and IHC results

Molecular subtype by FISH	Patient	Age	Sex	Hans type	Co-expression	Concordant FISH and NGS in *MYC* rearrangements	Concordant FISH and NGS in *BCL2* rearrangements	Concordant FISH and NGS in *BCL6* rearrangements	FISH-MYC	DNA_MYC	The number of supporting DNA reads	RNA_MYC	The number of supporting RNA reads	IHC-MYC	FISH-BCL2(partner)	DNA_BCL2	The number of supporting DNA reads	RNA_BCL2	The number of supporting RNA reads	IHC-BCL2	FISH-BCL6	DNA_BCL6	The number of supporting DNA reads	RNA_BCL6	The number of supporting RNA reads	IHC-BCL6
	p002	39	F	GCB	Yes	No	Yes	Yes	+	-		-		>80%	+(IGH)	BCL2::IGHJ6	303	BCL2::IGHD	56	100%	-	-		-		-
	p003	51	F	GCB	Yes	No	Yes	Yes	+	-		-		90%	+	BCL2::IGHJ6	359	BCL2::IGHJ6	422	100%	-	-		-		40%
	p010	70	F	GCB	Yes	No	Yes	No	+	-		-		50%	+(IGH)	IGHD3-10::intergenic(PHLPP1,BCL2)	65			100%	+	-		-		70%
DLBCL/HGBCL-*MYC*/*BCL2*	p023	58	F	GCB	Nb	No	Yes	No	+	-		-		30%	+(IGH)	BCL2::IGHJ6	1166	BCL2::IGHJ6	1940	90%	+	-		-		60%
	p001	48	F	GCB	Yes	Yes	Yes	Yes	+	PLEKHF2::*MYC*	368	-		80%	+	intergenic(PHLPP1,BCL2)::IGHJ6	67			90%	-	-		-		Diffuse +
	p004	66	F	GCB	Yes	Yes	Yes	Yes	+	-		BACH2::MYC	2000	80%	+(IGH)	IGHD3-10::BCL2	313	BCL2::IGHG1	45	>95%	-	-		-		-
	p009	65	F	GCB	Yes	Yes	Yes	Yes	+	IGHG1::MYC	31	-		45%	+(IGH)	IGHD3-9::intergenic(PHLPP1,BCL2)	175	BCL2::intergenic(IGHG4,IGHG2)	166	100%	+	IGHD::BCL6	366	intergenic(IGHG3,IGHD)::BCL6	739	2+
	p005	42	F	NGCB	Yes	No	Yes	No	+	-		-		50%	-	-		-		100%	+	-		-		80%
	p006	68	F	NGCB	Yes	Yes	Yes	Yes	+	IGHD::MYC	185	MYC::intergenic(IGHG3,IGHD)	179	90%	-	-		-		90%	+	-		intergenic(IGHM,IGHG6)::BCL6	479	95%
	p007	50	F	NGCB	Yes	Yes	Yes	Yes	+	IGHG1::MYC	211	MYC::intergenic(IGHG3,IGHD)	535	50%	-	-		-		100%	+	intergenic(MIR4537,IGHJ6)::BCL6	12	IGHJ6::BCL6	495	80%
	p008	47	F	GCB	Yes	Yes	Yes	Yes	+	intergenic(MIR4537,IGHJ6)::MYC	360	IGHD::MYC	84	80%	-	-		-		>90%	+	RCC1::BCL6	539	RCC1::BCL6	844	90%
	p011	61	M	GCB	Nb	Yes	Yes	Yes	+	IGH@2::MYC	6	IGHA2::MYC	74	95%	-	-		-		-	+	IGHA1::BCL6	107	-		3+
	p012	55	M	GCB	Yes	Yes	Yes	No	-	-		-		40%	+	intergenic(PHLPP1,BCL2)::IGHJ6	249	-		100%	-	EIF4A2::BCL6	203	EIF4A2::BCL6	1010	80%
	p013	47	M	GCB	Nb	Yes	Yes	Yes	-	-		-		80%	+(IGH)	BCL2::IGHJ6	261	BCL2::IGHG6	280	-	-	-		-		90%
	p014	81	M	NGCB	Yes	Yes	Yes	Yes	-	-		-		80%	-	-		-		90%	+	LPP::BCL6	263	-		90%
	p015	68	M	GCB	Yes	Yes	Yes	Yes	-	-		-		80%	-	-		-		100%	+	intergenic(MIR4537,IGHJ6)::BCL6	16	IGHJ6::BCL6	134	80%
	p016	51	M	GCB	Yes	Yes	Yes	Yes	-	-		-		60%	-	-		-		90%	+	GAS5::BCL6	634	-		70%
	p017	72	F	NGCB	Yes	Yes	Yes	Yes	-	-		-		50%	-	-		-		80%	+	BCL6::HSP90AA1	60	HSP90AA1::BCL6	19	50%
	p018	51	M	NGCB	Yes	Yes	Yes	Yes	-	-		-		80%	-	-		-		>95%	+	intergenic(BCL6,LINC01991)::BCL6	67	LCP1::BCL6	453	80%
	p019	24	F	NGCB	Yes	Yes	Yes	Yes	-	-		-		70%	-	-		-		70%	+	IGHA1::BCL6	218	BCL6::IGHA1	575	90%
DLBCL, NOS	p020	56	M	GCB	Yes	Yes	Yes	Yes	-	-		-		40%	-	-		-		90%	+	IGHG1::BCL6	47	intergenic(IGHG3,IGHD)::BCL6	619	3+
	p021	74	M	NGCB	Yes	Yes	Yes	No	-	-		-		50%	-	-		-		60%	+	-		-		80%
	p022	36	F	NGCB	Yes	Yes	Yes	No	-	-		-		40%	-	-		-		100%	+	-		-		1+
	p024	63	F	GCB	Nb	Yes	Yes	Yes	-	-		-		30%	-	-		-		-	-	-		-		80%
	p025	65	F	NGCB	Nb	Yes	Yes	Yes	-	-		-		30%	-	-		-		95%	-	-		-		70%
	p026	81	M	NGCB	Nb	Yes	Yes	Yes	-	-		-		30%	-	-		-		90%	-	-		-		50%
	p027	62	M	NGCB	Nb	Yes	Yes	Yes	-	-		-		30%	-	-		-		95%	-	-		-		1+
	p028	74	F	GCB	Nb	Yes	Yes	Yes	-	-		-		30%	-	-		-		20%	-	-		-		60%
	p029	70	F	NGCB	Nb	Yes	Yes	Yes	-	-		-		3%	-	-		-		95%	-	-		-		<10%
	p030	67	F	GCB	Nb	Yes	Yes	Yes	-	-		-		10%	-	-		-		90%	-	-		-		40%
	p031	60	F	NGCB	Nb	Yes	Yes	Yes	-	-		-		30%	-	-		-		80%	-	-		-		30%
	p032	78	M	GCB	Nb	Yes	Yes	Yes	-	-		-		10%	+(IGH)	intergenic(PHLPP1,BCL2)::IGHJ2	139	-		>90%	-	-		-		>90%
	p033	67	M	NGCB	Nb	Yes	Yes	Yes	-	-		-		30%	-	-		-		>90%	-	-		-		30%
	p034	68	M	NGCB	Nb	Yes	Yes	Yes	-	-		-		20%	-	-		-		80%	+	IGHG1::BCL6	203	intergenic(IGHG1,IGH33)::BCL6	724	85%

FISH, fluorescence in situ hybridization; NGS, integrated DNA- and RNA-sequencing; IHC, immunohistochemistry; GCB, germinal-center B-cell like; NGCB, non-germinal-center B-cell like; F, female; M, male; DLBCL/HGBL-*MYC*/*BCL2*, diffuse large B-cell lymphoma/high-grade B-cell lymphoma with MYC and BCL2 rearrangements; NOS, not otherwise specified.

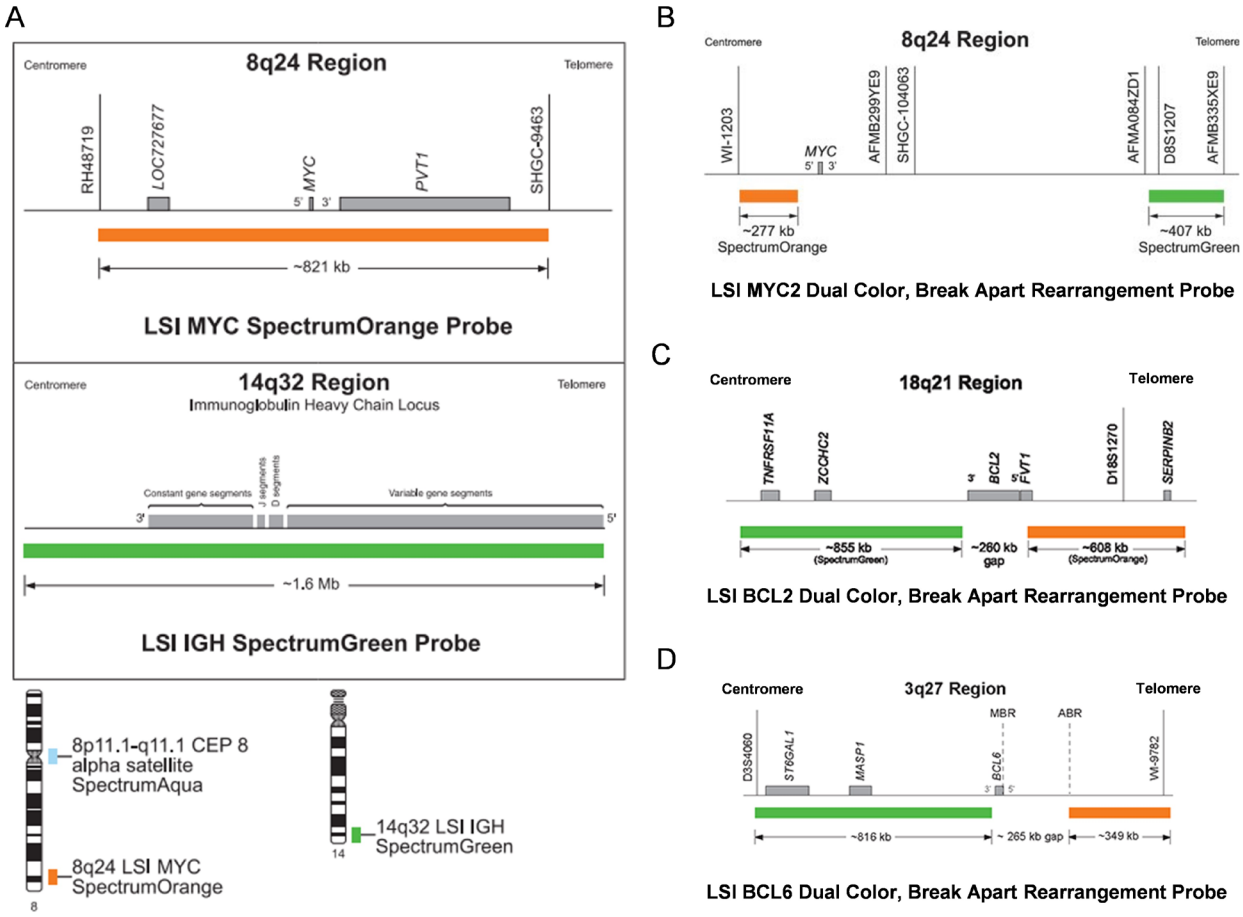

Supplementary Figure S2. Schematic diagram for the FISH probes. A) Dual fusion probes for *IGH::MYC*; B) *MYC* break-apart probe; C) *BCL2* break-apart probe; D) *BCL6* break-apart probe.

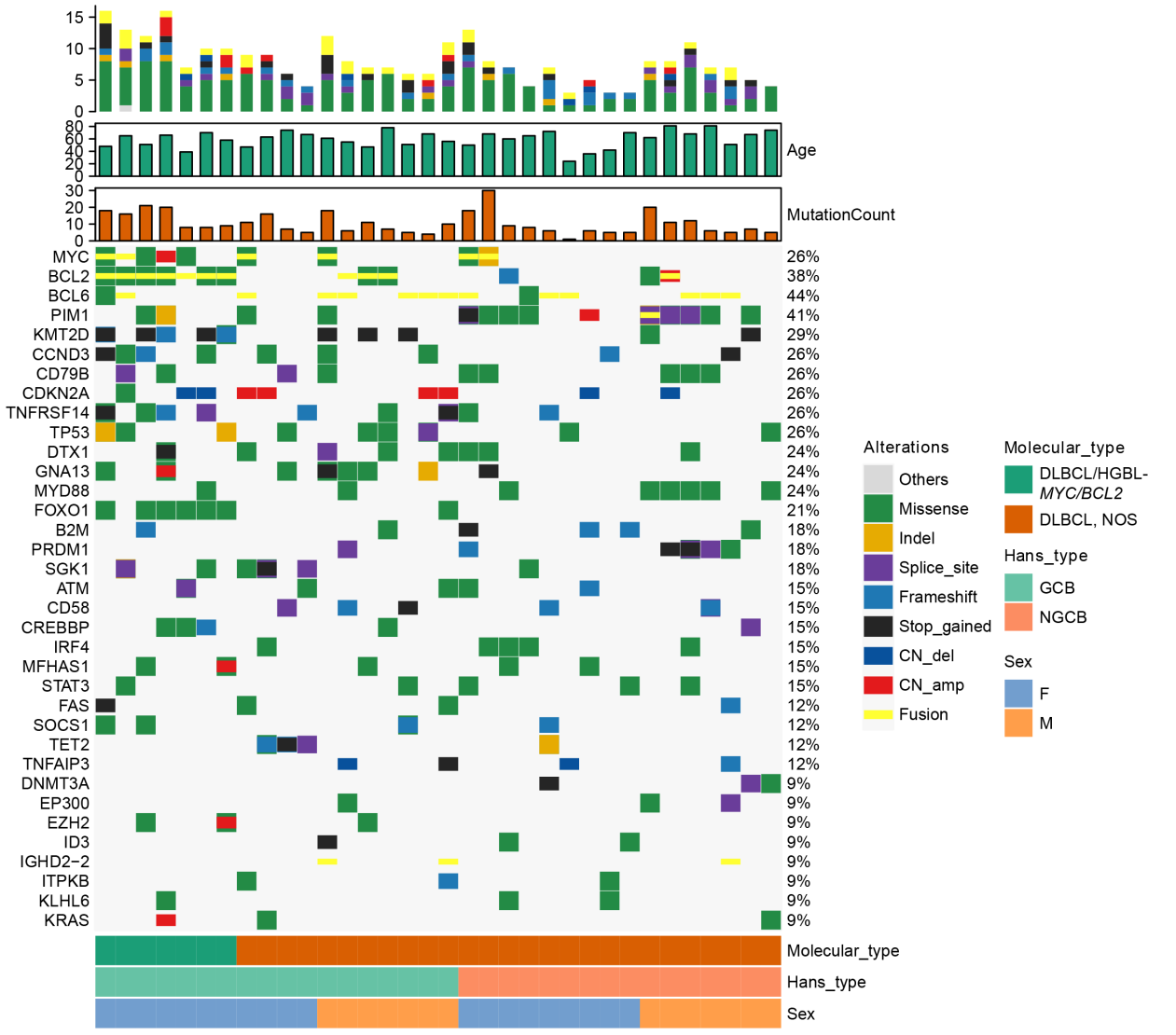

Supplementary Figure S3. Molecular alterations detected with DNA-sequencing in patients. Abbreviations: DLBCL-diffuse large B-cell lymphoma; GCB-germinal-center B-cell-like; NGCB-non-germinal-center B-cell-like; Indel-insertion and deletion; CN-copy number; F-female; M-male; DLBCL/HGBCL-*MYC/BCL2*-diffuse large B-cell lymphoma/high-grade B-cell lymphoma with *MYC* and *BCL2* rearrangements; NOS-not otherwise specified

A

	FISH	
DNA-sequencing	*MYC*+	*MYC*-
MYC+	6	0
MYC-	6	22
	Sensitivity=50%	Specificity=100%
RNA-sequencing		
MYC+	5	0
MYC-	7	22
	Sensitivity=41.7%	Specificity=100%

B

	FISH	
DNA-sequencing	*BCL2*+	*BCL2*-
BCL2+	10	0
BCL2-	0	24
	Sensitivity=100%	Specificity=100%
RNA-sequencing		
BCL2+	6	0
BCL2-	4	24
	Sensitivity=60%	Specificity=100%

C

	FISH	
DNA-sequencing	*BCL6*+	*BCL6*-
BCL6+	12	1
BCL6-	6	15
	Sensitivity=66.7%	Specificity=93.8%
RNA-sequencing		
BCL6+	10	1
BCL6-	8	15
	Sensitivity=55.6%	Specificity=93.8%

Supplementary Figure S4. Performance of DNA- or RNA- sequencing in detecting rearrangements. A, *MYC* rearrangement; B, *BCL2* rearrangement. FISH, fluorescence *in situ* hybridization.

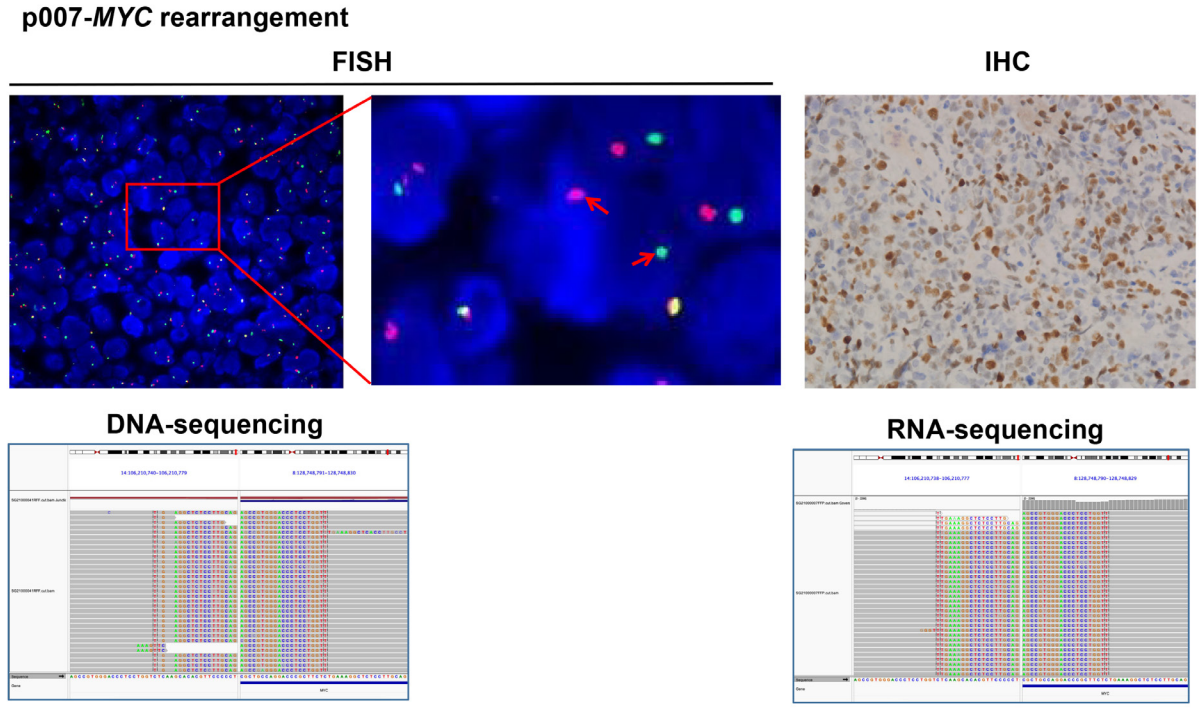

Supplementary Figure S5. Representative images with concordant FISH and integrated NGS sequencing in detecting *MYC* rearrangement. *MYC* fusion in p007 was detectable by FISH, IHC, DNA-, and RNA-sequencing. Red arrows and brown color indicate the presence of *BCL2* fusions and BCL2 expression detected by FISH and IHC (×400), respectively. The integrative genomics viewer screenshots reveal the presence of *MYC* fusions. FISH, fluorescence *in situ* hybridization; IHC, immunohistochemistry; NGS, next-generation sequencing.

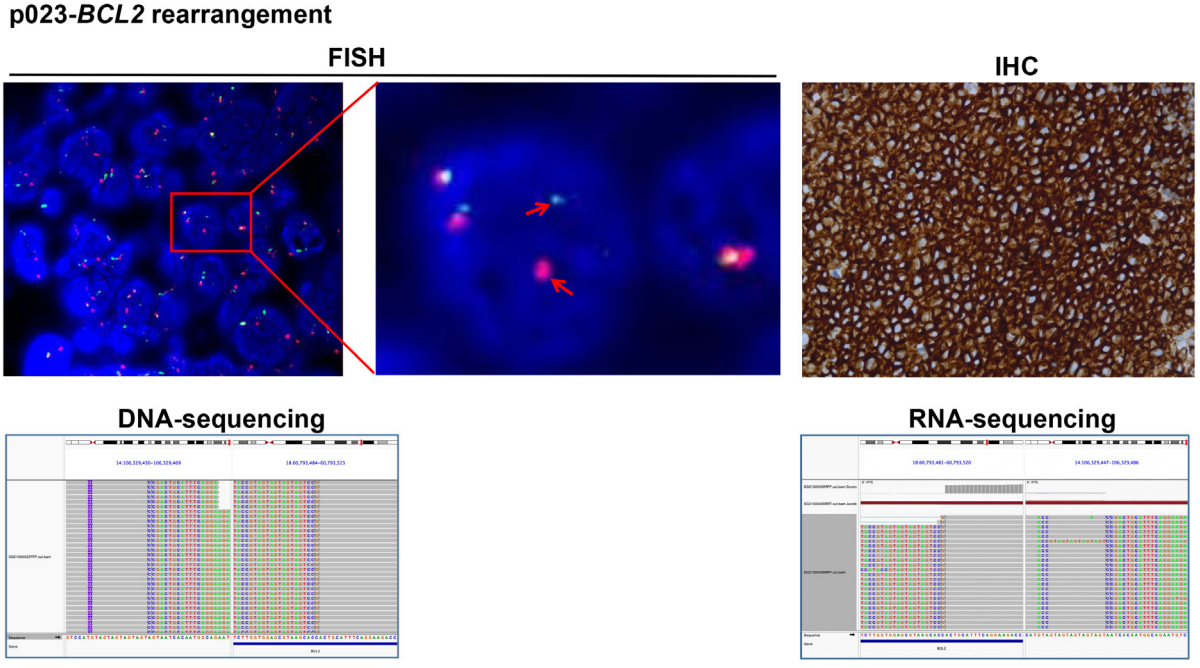

Supplementary Figure S6. Representative images with concordant FISH and integrated NGS sequencing in detecting *BCL2* rearrangement. *BCL2* fusion in p023 was identified by FISH, IHC, DNA-, and RNA-sequencing. Red arrow and brown color indicate the presence of *BCL2* fusions and BCL2 expression detected by FISH and IHC (×400), respectively. The integrative genomics viewer screenshots reveal the presence of *BCL2* fusions. Abbreviations: FISH-fluorescence *in situ* hybridization; IHC-immunohistochemistry; NGS-next-generation sequencing.

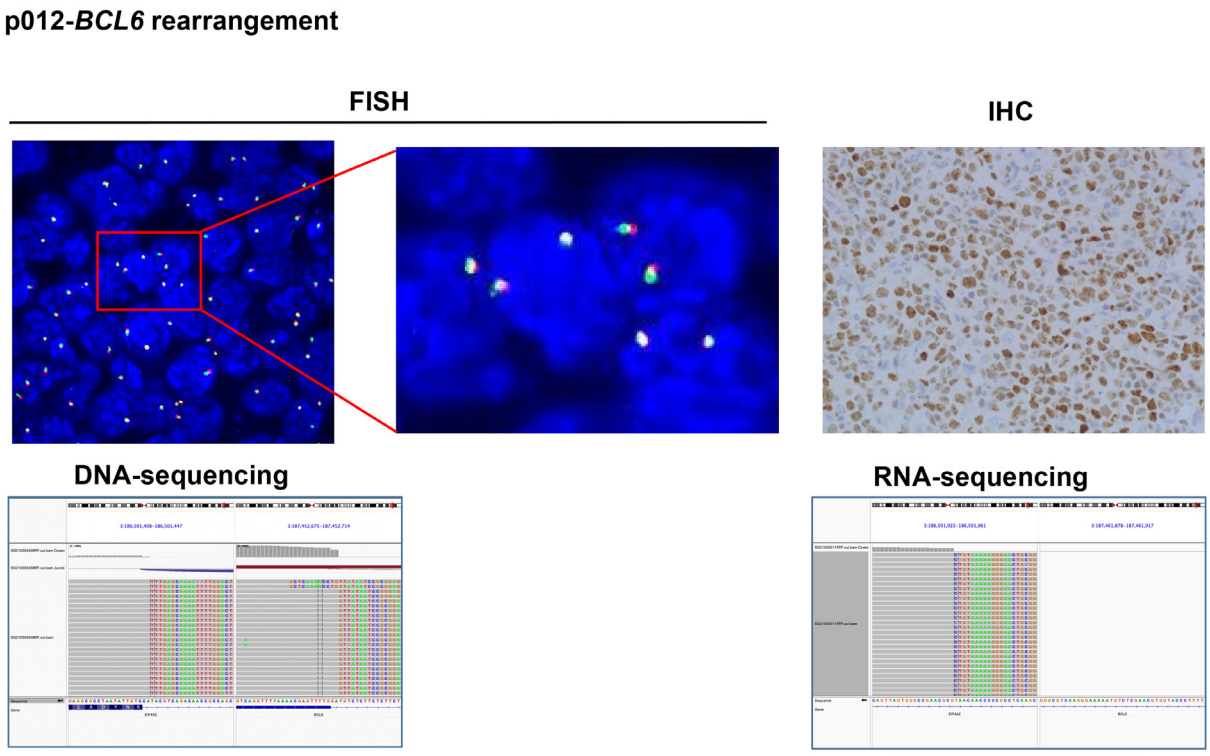

Supplementary Figure S7. Representative images with discordant FISH and integrated NGS sequencing in detecting *BCL6* rearrangements. *BCL6* fusion in p012 was negative by FISH but positive by IHC, DNA-, and RNA-sequencing. Brown color indicates the BCL6 expression detected by IHC (×400). Integrative genomics viewer screenshots reveal the presence of *BCL6* fusions. Abbreviations: FISH-fluorescence *in situ* hybridization; IHC-immunohistochemistry; NGS-next-generation sequencing.